

# Secretory Carcinoma of the Skin

## Report of 6 Cases, Including a Case With a Novel *NFIX-PKN1* Translocation

Liubov Kastnerova, MD,\*† Boštjan Luzar, MD, PhD,‡ Keisuke Goto, MD,§¶##\*\*  
 Viktor Grishakov MD,†† Zoran Gatalica, MD,‡‡ Jivko Kamarachev, MD,§§  
 Petr Martinek, PhD,\*† Veronika Hájková, MSc,† Petr Grossmann, PhD,\*†  
 Hiroshi Imai, MD, PhD,|| Hideaki Fukui, MD,¶¶ Michal Michal, MD,\*† and  
 Dmitry V. Kazakov, MD, PhD\*†

**Abstract:** Secretory carcinoma of the skin is a rare adnexal carcinoma, which is morphologically and immunohistochemically identical to secretory carcinoma of the breast and is associated with the presence of t(12;15) translocation, resulting in the *ETV6-NTRK3* gene fusion. Nineteen cases of primary cutaneous secretory carcinoma have been previously published in the literature. In this study, we describe 6 new cases of secretory carcinoma of the skin. The study group consisted of 5 female patients and 1 male patient, ranging in age from 57 to 98 years (mean: 74.2, median: 74). Locations included the axilla (2), neck, eyelid, thigh, and nipple base, each one. Microscopically, all but 1 tumor were well circumscribed and nonencapsulated and exhibited characteristic abundant secretions within the microcystic and tubular spaces comprised by bland oval, round to cuboidal neoplastic cells. In addition, solid areas and focal pseudopapillae were seen, and, in 1 case, a focal mucinous component with small lakes of mucin containing small tumor nests or tubules of the neoplastic cells was present. The remaining neoplasm was mostly solid and papillary, with only few characteristic lumina containing secretions. Immunohistochemically, all cases expressed S-100 protein, mammaglobin, STAT5, GATA3,

and NTRK. *ETV6-NTRK3* gene fusion was detected in 5 cases, whereas, in the remaining tumor, a novel *NFIX-PKN1* gene fusion was found.

**Key Words:** secretory carcinoma, mammary analog secretory carcinoma, adnexal neoplasms, *ETV6-NTRK3*, *NFIX-PKN1*, fusion

(*Am J Surg Pathol* 2019;43:1092–1098)

Primary cutaneous secretory carcinoma is a rare adnexal carcinoma that is histopathologically identical to homologous neoplasms in the salivary gland and breast.<sup>1–7</sup> It was recognized in the skin in 2009.<sup>8</sup> Since then, 19 cases have been reported, mostly as isolated case reports, with only a small series of 6 cases.<sup>2,8–19</sup> In addition to the distinctive histopathologic appearances, cutaneous secretory carcinoma seems to be associated with the characteristic balanced t(12;15) (p13; q25) *ETV6-NTRK3* translocation, akin to their mammary and salivary gland counterparts.<sup>2</sup> Herein, we report a series of 6 new cases of secretory carcinoma of the skin, including new microscopic features and a novel *NFIX-PKN1* translocation.

## MATERIAL AND METHODS

### Case Selection

Six cases of secretory carcinoma of the skin were identified, prospectively or retrospectively, in the consultation and institutional databases of the authors (2009–2018). None of the cases was previously published. Follow-up information was provided by attending physicians.

### Immunohistochemical Studies

Immunohistochemical staining was performed on 4- $\mu$ m-thick sections, cut from formalin-fixed, paraffin-embedded tissue, using a Ventana BenchMark XT automated stainer (Ventana Medical Systems, Tucson, AZ), according to the manufacturer's protocol.

The following antibodies were used: S-100 protein (polyclonal; RTU; Ventana), STAT5 (E289, 1:500, AbCam), mammaglobin (clone 304-1A5; RTU; DakoCytomation),

From the \*Sikl's Department of Pathology, Medical Faculty in Pilsen, Charles University in Prague; †Bioptical Laboratory, Pilsen, Czech Republic; ‡Institute of Pathology, Medical Faculty University of Ljubljana, Ljubljana, Slovenia; ††Department of Pathology, Moscow City Oncology Hospital №62, Moscow, Russia; ‡‡Department of Pathology, Caris Life Sciences, Phoenix, AZ; §Department of Pathology, Tokyo Metropolitan Cancer and Infectious Disease Center Komagome Hospital; ||Department of Pathology, Itabashi Central Clinical Laboratory, Tokyo; ¶Department of Diagnostic Pathology, Shizuoka Cancer Center Hospital, Nagaizumi; #Department of Diagnostic Pathology and Cytology, Osaka International Cancer Institute, Osaka; \*\*Department of Dermatology, Hyogo Cancer Center, Akashi; |||Pathology Division, Mie University Hospital, Tsu; ¶¶Department of Surgical Pathology, Hokkaido University Hospital, Sapporo, Japan; and §§Department of Dermatology, University Hospital Zurich, Zurich, Switzerland.

Conflicts of Interest and Source of Funding: Supported in part by a Charles University project (SVV 260 391/2018). The authors have disclosed that they have no relationship with, or financial interest in, any commercial companies pertaining to this article.

Correspondence: Dmitry V. Kazakov, MD, Sikl's Department of Pathology, Charles University Medical Faculty Hospital, Alej Svobody 80, Pilsen 304 60, Czech Republic (e-mail: kazakov@medima.cz).  
 Copyright © 2019 Wolters Kluwer Health, Inc. All rights reserved.

NTRK (A7H6R, 1:25; Cell Signaling), GATA3 (clone L50-823; 1:200; BioCareMedical), CK7 (clone OV-TL 12/30; 1:200; DakoCytomation), TTF-1 (8G7G3/1, 1:100, Dako), p63 (clone 4A4; RTU; Ventana), and CD117 (polyclonal, 1:800, Dako). The panel varied between individual cases depending on the origin.

## Molecular Genetic Studies and Fluorescence In Situ Hybridization

### Detection of *ETV6-NTRK3* Fusion and *NFIX-PKNI* Fusion Transcript by Reverse Transcription Polymerase Chain Reaction

RNA was extracted using the RecoverAll Total Nucleic Acid Isolation Kit (Ambion, Austin, TX). cDNA was synthesized using the Transcriptor First Strand cDNA Synthesis Kit (RNA input 500 ng) (Roche Diagnostics). All procedures were performed according to the manufacturer's protocols. Amplification of a 105 bp product and a 133 bp product of the  $\beta$ 2-microglobulin gene, and a 247 bp product of the *PGK* gene, was used to test the quality of the extracted RNA, as previously described.<sup>20–22</sup>

For polymerase chain reaction (PCR), 2  $\mu$ L of cDNA was added to the reaction, which consisted of 12.5  $\mu$ L of HotStar Taq PCR Master Mix (Qiagen, Hilden, Germany), 10 pmol of each primer, and distilled water up to 25  $\mu$ L.<sup>23,24</sup> The amplification program comprised denaturation at 95°C for 14 minutes followed by 45 cycles of denaturation at 95°C for 1 minute; annealing at temperatures 60°C was carried out for 1 minute and extension at 72°C for 1 minute. The procedure was completed by incubation at 72°C for 7 minutes.

Successfully amplified PCR product was purified with magnetic particles using Agencourt AMPure (Agencourt Bioscience Corporation, A Beckman Coulter Company, Beverly, MA). The product was then bidirectionally sequenced using Big Dye Terminator Sequencing Kit (PE/Applied Biosystems, Foster City, CA) and purified with magnetic particles using Agencourt CleanSEQ (Agencourt Bioscience Corporation); all this was carried out according to the manufacturer's protocols and run on an automated sequencer ABI Prism 3130x1 (Applied Biosystems) at a constant voltage of 13.2 kV for 11 minutes.

### Detection of *ETV6* and *NTRK3* by Fluorescence In Situ Hybridization Method

Four- $\mu$ m-thick FFPE sections were placed onto positively charged slides. Hematoxylin and eosin-stained slides were examined for determination of areas for cell counting. The unstained slides were routinely deparaffinized and incubated in the 1 $\times$  Target Retrieval Solution Citrate pH 6 (Dako, Glostrup, Denmark) at 95°C/40 minutes and subsequently cooled for 20 minutes at room temperature in the same solution. The slides were washed in deionized water for 5 minutes, and they were digested in protease solution with Pepsin (0.5 mg/mL) (Sigma Aldrich, St Louis, MO) in 0.01 M HCl at 37°C/25 to 60 minutes, according to the sample conditions. The slides were then placed in deionized water for 5 minutes, dehydrated in a series of ethanol solution (70%, 85%, and 96% for 2 min each), and air-dried.

For the detection of *ETV6* rearrangement, a commercial probe, Vysis ETV6 Break Apart FISH Probe Kit (Vysis/Abbott Molecular, Illinois), was used. The ETV6 probe was mixed with water and LSI/WCP (Locus-Specific Identifier/Whole Chromosome Painting) hybridization buffer (Vysis/Abbott Molecular) in a 1:2:7 ratio, respectively. The probe for the detection of the rearrangement of the *NTRK3* gene region was mixed from custom-designed SureFISH probes (Agilent Technologies Inc., Santa Clara, CA). Chromosomal regions for *NTRK3* break-apart probe oligos are chr15:87501469-88501628 and chr15:88701444-89700343. The probe mixture was prepared from corresponding probes (each color was delivered in a separated well), deionized water, and LSI Buffer (Vysis/Abbott Molecular) in a 1:1:1:7 ratio, respectively. An appropriate amount of mixed probe was applied on specimens, covered with a glass coverslip, and sealed with rubber cement. The slides were incubated in the ThermoBrite instrument (StatSpin/Iris Sample Processing, Westwood, MA) with co-denaturation at 85°C/8 minutes and hybridization at 37°C/16 hours. The rubber-cemented coverslip was then removed, and the slide was placed in the post-hybridization wash solution (2 $\times$ SSC/0.3% NP-40) at 72°C/2 minutes. The slide was air-dried in the dark, counterstained with 4', 6'-diamidino-2-phenylindole (DAPI; Vysis/Abbott Molecular), coverslipped, and immediately examined.

The sections were examined with an Olympus BX51 fluorescence microscope (Olympus Corporation, Tokyo, Japan) using a  $\times$ 100 objective and the filter sets Triple Band Pass (DAPI/SpectrumGreen/SpectrumOrange), Dual Band Pass (SpectrumGreen/SpectrumOrange), and Single Band Pass (SpectrumGreen or SpectrumOrange).

For each probe, 100 randomly selected nonoverlapping tumor cell nuclei were examined for the presence of yellow or green and orange fluorescent signals. Yellow signals were considered negative, and separate orange and green signals were considered as positive. Cutoff values were set to >10% of nuclei with chromosomal breakpoint signals (mean, +3 SD in normal non-neoplastic control tissues).

### Detection of *ETV6-NTRK3* and *NFIX-PKNI* Fusion Transcripts by Next-generation Sequencing

For next-generation sequencing (NGS) studies, 2 to 3 FFPE sections (10  $\mu$ m thick) were macrodissected to isolate tumor-rich regions. The samples were extracted for total nucleic acid using Agencourt FormaPure Kit (Beckman Coulter, Brea, CA), following the corresponding protocol with overnight digestion and an additional 80°C incubation, as described in the modification of the protocol by ArcherDX (ArcherDX Inc., Boulder, CO).

Total nucleic acid was quantified using the Qubit Broad Range RNA Assay Kit (Thermo Fisher Scientific) and 2  $\mu$ L of sample.

### RNA Integrity Assessment and Library Preparation for NGS

Unless otherwise indicated, 250 ng of FFPE RNA was used as input for NGS library construction. To assess RNA quality, the PreSeq RNA QC Assay using iTaq Universal SYBR Green Supermix (Biorad, Hercules, CA)

was performed on all samples during library preparation to generate a measure of the integrity of RNA (in the form of a cycle threshold [Ct] value). Library preparation and RNA QC were performed following the Archer Fusion Plex Protocol for Illumina (ArcherDX Inc.). The Archer FusionPlex Solid Tumor Kit (covering 53 genes) was used. Final libraries were diluted 1:100,000 and quantified in a 10 µL reaction following the Library Quantification for Illumina Libraries protocol and assuming a 200 bp fragment length (KAPA, Wilmington, MA). The concentration of final libraries was around 200 nM. Threshold representing the minimum molar concentration for which sequencing can be robustly performed was set at 50 nM.

**NGS Sequencing and Analysis**

Libraries were sequenced on a NextSeq. 500 sequencer (Illumina, San Diego, CA). They were diluted to 4 nM, and equal amounts of up to 30 libraries were pooled per run. The optimal number of raw reads per sample was set to 3,000,000. Library pools were diluted to 1.8 pM library stock spiked with 20% PhiX and loaded in the NextSeq MID cartridge. Analysis of sequencing results was performed using the Archer Analysis software (v5.1.7; ArcherDX Inc.). Fusion parameters were set to a minimum of 5 valid fusion reads with a minimum of 3 unique start sites within the valid fusion reads.

**RESULTS**

**Clinical Features**

There were 5 female patients and 1 male patient, with ages ranging at diagnosis from 57 to 98 (mean: 74.2, median: 74). Location included axilla (n=2), neck (n=1), eyelid (n=1), thigh (n=1), and nipple base (n=1). All skin tumors occurred as solitary nodules (Fig. 1). The patient with the lesion involving the nipple was a 75-year-old woman, who noticed uncomfortable rash to her right breast, above the nipple, for 2 months, with nipple protrusion. Her mammograms and breast ultrasound were negative at that time but magnetic



**FIGURE 1.** Case 4. A 15×10 mm slowly growing (8 mo) painless nodule on the lower eyelid.

**TABLE 1.** Summary of the Main Features

Case	Sex/ Age (y)	Location/ Clinical Diagnosis	Treatment/Follow-up	Histology Mitosis (mm <sup>2</sup> )	Size (mm)*	Immunohistochemistry	Fusion	FISH ba	Molecular-genetic Study	
									RT-PCR	NGS
1	F/75	Axilla/tumor	Excision. Reexcision within a month, then NED at 12 mo	Typical 4/mm <sup>2</sup>	7	S-100+, STAT5+, MGA+, NTRK+, GATA3+	ETV6-NTRK3	+	+	+
2	F/98	Axilla/tumor	Excision. NED at 2 mo, later lost to follow-up	Typical 1/mm <sup>2</sup>	6	S-100+, STAT5+, MGA+, NTRK+	ETV6-NTRK3	+	-	+
3	F/67	Neck/tumor	Excision/NED 32 mo	Typical 0/mm <sup>2</sup>	4	S-100+/-, STAT5+, MGA+, NTRK+, GATA3+	ETV6-NTRK3	ND	+	ND
4	M/73	Right lower eyelid/tumor	Excision/NED 6 mo	More solid, with true papillae and blastoid cells 2/mm <sup>2</sup>	14	S100+, MGA+/, GATA3+, CD117+, TTF1-STAT5+/-, NTRK+	ETV6-NTRK3	+	ND	+
5	F/57	Left thigh/tumor	Excision/NED 14 mo	Mucinous component 4/mm <sup>2</sup>	7	S-100+, STAT5+, MGA+, CK7+, GATA3+/- p63+/-, CD117-	NFIX-PKNI	ND	+	+
6	F/75	Nipple base /rash	Right central partial mastectomy /mts to 1 of 15 axillary LN	Typical 0/mm <sup>2</sup>	6	S100+, STAT5+, MGA+, NTRK+	ETV6-NTRK3	+	ND	+

\*Size is measured on the microscopic slides. ba indicates break apart; FISH, fluorescence in situ hybridization; LN, lymph nodes; MGA, mammaglobin; ND, not done; NED, not evidence of disease.

resonance imaging was suspicious for malignancy in a right axillary lymph node, which was biopsied and turned positive for metastatic adenocarcinoma of a probable breast origin, with the following phenotype ER-, PR-, HER2-neu-, Ki-67 - 5%. A punch biopsy of the right nipple lesion was performed, and the diagnosis of secretory carcinoma was established on the basis of detection of *ETV6-NTRK3* fusion. Subsequent PET/CT revealed a hypermetabolic spot in the area of the seventh left rib. The patient had a history of a sixth left rib fracture about a year ago that was said to be due to a fall. There was a question whether the PET activity was due to the previous trauma or represented a metastatic disease. Finally, right central partial mastectomy was performed. No tumor in the breast parenchyma was found. In the other 5 cases, all neoplasms were surgically excised, with a conventional elliptical excision. In one case, reexcision was performed. None of these patients had evidence of disease (follow-up ranged from 2 to 32 mo) (Table 1).

### Histopathologic Features

Of the 6 lesions, 5 manifested typical features with characteristic abundant intraluminal secretions within closely packed microcystic and tubular spaces comprised of bland oval, round to cuboidal neoplastic cells. In addition, solid areas and focal pseudopapillae were seen. When assessable, most tumors were relatively well circumscribed, nonencapsulated, and confined to the dermis (Fig. 2).

In one case (case 5), there was a focal mucinous component which was less regular and extended focally into the subcutis. It was composed of small lakes of

mucin-containing tubules of the neoplastic cells or small tumor nests. Mucinous lacunae were often seen at the periphery of the intact tubules that gradually disappeared. Rare tubules contained a preserved peripheral basal/myoepithelial cell layer, likely representing an in situ lesion or preexisting eccrine/apocrine duct (Fig. 3). Another lesion containing an in situ component was the tumor from the nipple.

The lesion from the eyelid (case 4) was mostly solid and papillary, showing both micropapillae and true papillae with a fibrous core; characteristic lumina containing secretions were less conspicuous in comparison with the other 5 neoplasms. There also were variably sized lumina (some markedly distended) with apocrine or colloid-like secretion. Focally, the cells in this neoplasm assumed hobnail appearances, and there were areas with larger “blastoid” cells, but no high-grade atypia was evident (Fig. 4).

In no case was ulceration of the epidermis, perineural invasion, and lymphovascular involvement found. In neither axillary cases was there any evidence of residua of mammary tissue. The mitotic rate ranged from 0 to 4 mm<sup>2</sup>. The lymph node metastasis from the nipple lesion (case 6) was not available for histopathologic review.

### Immunohistochemical Findings

Neoplastic cells were positive for S-100 protein, mammaglobin, STAT5, GATA3, and NTRK. The neoplasm with a mucinous component (case 5) manifested some differences between the mucinous and conventional parts, namely S-100 protein was weak and focal in the main bulk of the tumor with the conventional appearance,

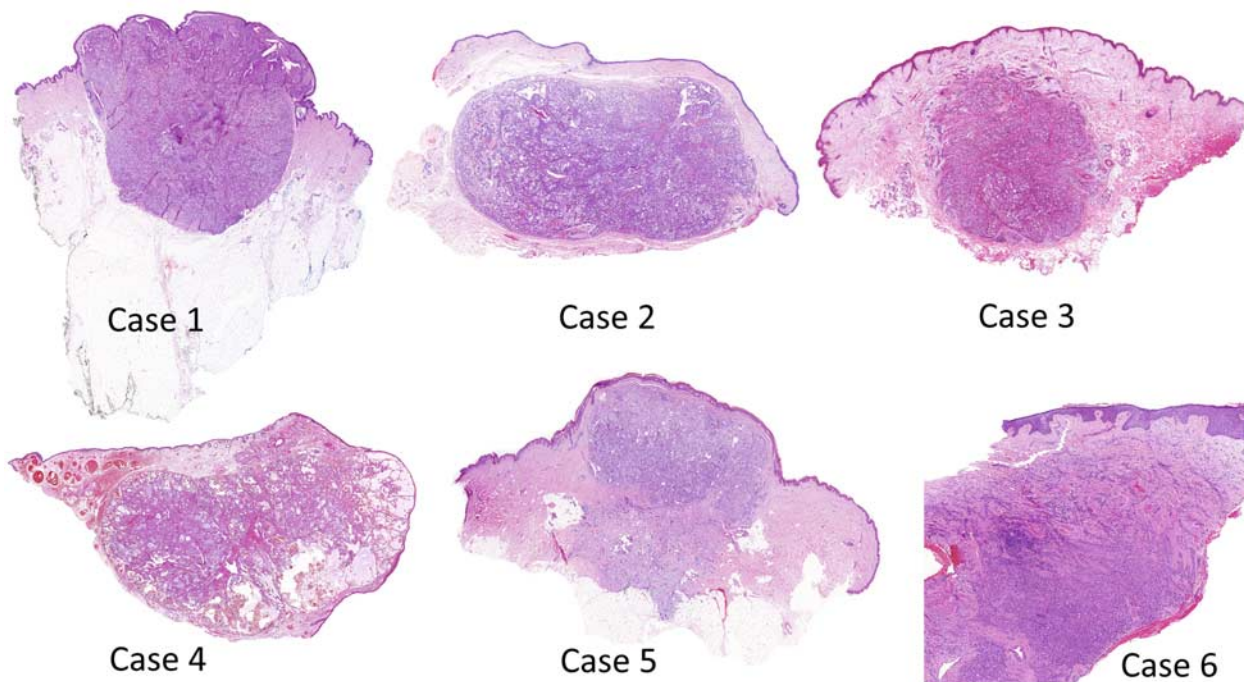


**FIGURE 2.** Whole-mount sections of 6 cases, 4 of which are well circumscribed. Case 4 shows a focal invasion into the subcutis, and the tumor on the nipple (case 6) has irregular outlines.

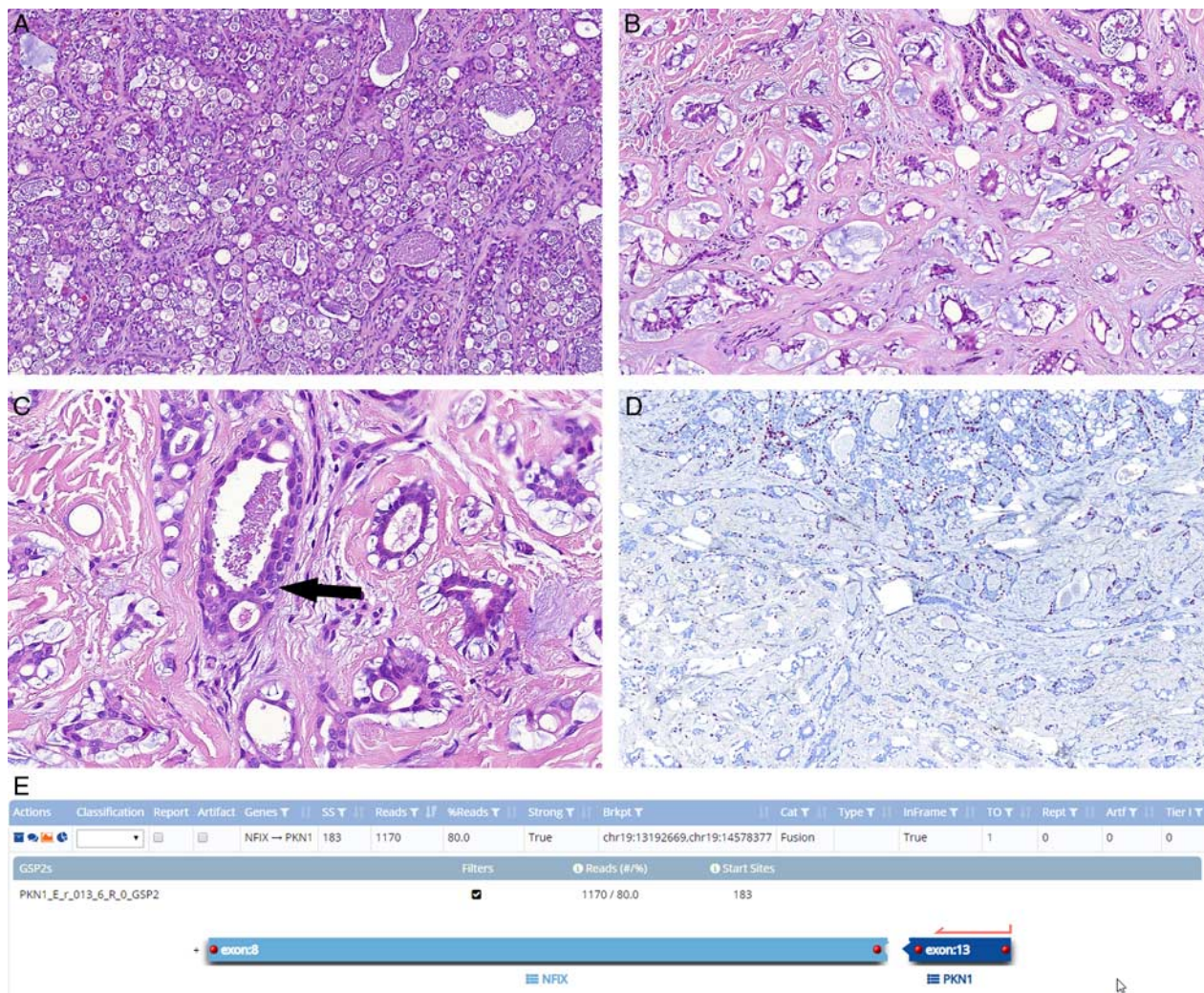


**FIGURE 3.** Secretory carcinoma with a novel *NFIX-PKN1* fusion (case 5). The typical appearance of closely packed microcysts and tubules lined by bland cells with characteristic abundant bubbly secretion (A). The mucinous component with small lakes of mucin, spilling into the surrounding dermis containing partly preserved or destroyed tubules. Note lacunae of the mucus located at the periphery of relatively intact tubules (B). The duct containing incipient secretions and intact peripheral basal/myoepithelial cell layer, likely representing preexisting apocrine/eccrine duct (an in situ lesion) (C, arrow). Positivity of p63 for the abluminal cells in the upper part of the tumor and loss of p63 expression in the mucinous areas (D). Screenshot from the Archer Analysis software, depicting the details of the detected *NFIX-PKN1* fusion: SS—the number of unique start sites supporting the event. Reads—the number of unique reads supporting the event. %Reads—the percent of reads supporting the event. Strong—True/False value indicating whether the Fusion has passed all Strong Evidence filters. Brkpt—True/False value indicating whether the Fusion has passed all Strong Evidence filters. InFrame—True/False/Unknown value indicating whether the event is predicted to be in-frame, and thus a functional transcript (E).

whereas diffuse positivity was seen in the mucinous moiety. There was also the loss of p63 in the mucinous areas compared with the conventional parts. The panel for each individual case is listed in Table 1.

### Gene Fusions

In 5 cases, *ETV6-NTRK3* translocation was detected, whereas, in the remaining case, a novel in-frame *NFIX-PKN1*, with breakpoints located in exon 8 of the *NFIX* gene and exon 13 of the *PKN1* gene, was found. The fusions were detected in 5 cases by NGS and confirmed by either

break-apart fluorescence in situ hybridization (FISH) or reverse transcription polymerase chain reaction (RT-PCR) in 4 and 3 cases, respectively. In one case, only RT-PCR was used to detect the translocation (Table 1). In case of the *NFIX-PKN1* fusion, it was impossible to use FISH break-apart probes for validation, inasmuch as the genes are located too close to one another.

### DISCUSSION

Our series extends the histopathologic spectrum of secretory carcinoma of the skin and the spectrum of its

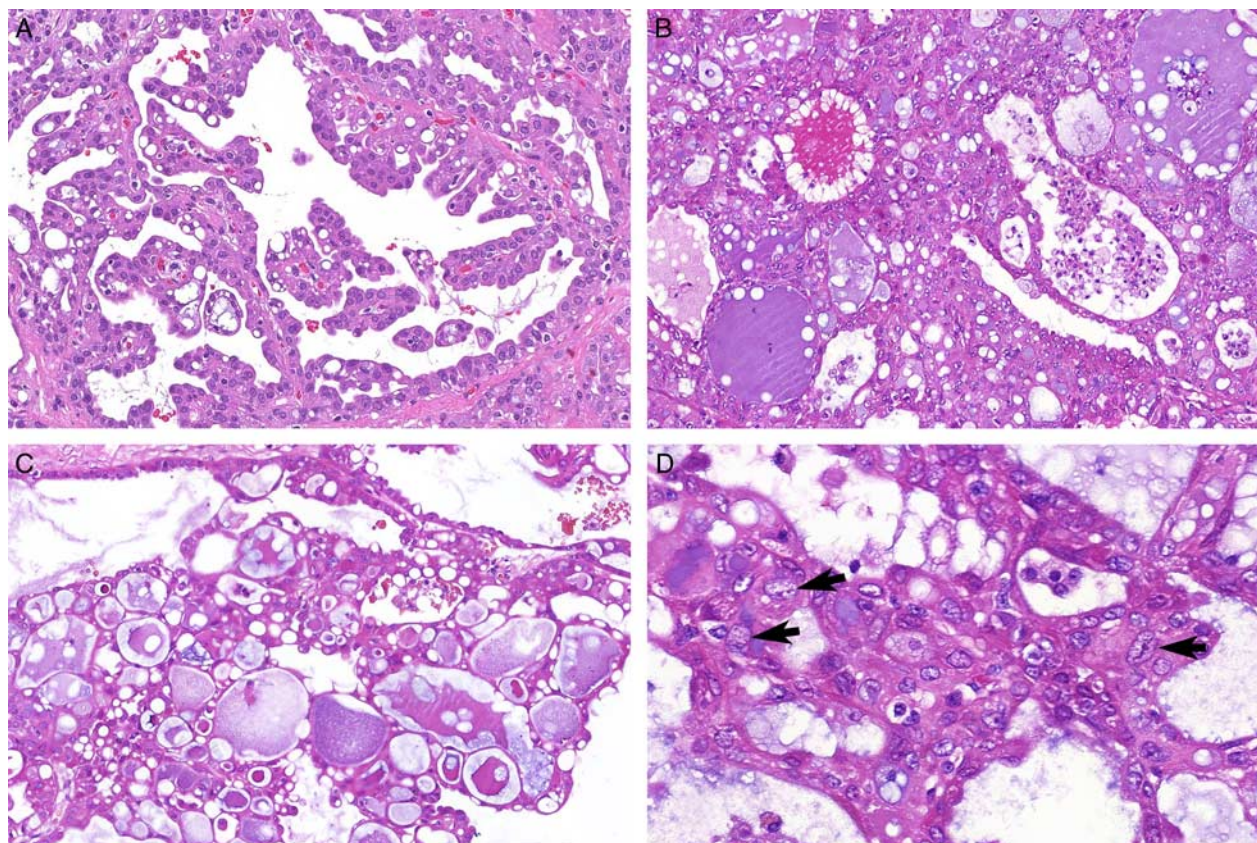


**FIGURE 4.** Secretory carcinoma of the eyelid (case 4). Numerous micropapillary structures and true papillae with a fibrous core within cystic spaces (A). The colloid-like (moth eaten) spaces with abundant secretion (B) and microcystic area containing abundant eosinophilic secretion (C). Atypical neoplastic cells with large nuclei (2 to 3 times larger than a majority of tumor cells) and pronounced nucleoli (D, arrows).

genetic alterations. Although most cases had typical histopathologic appearances, 2 cases are worthy of a short comment. In one case (case 5), in addition to conventional areas, there was a minor mucinous component, which has not been reported in skin lesions, to the best of our knowledge. However, a similar salivary gland tumor was included in the series of Skalova et al<sup>25</sup> (Fig. 2A). Notably, this mucinous component had slightly different immunophenotype from that in the main bulk of the lesion with respect to S-100 protein and p63 expression. Moreover, there were structures with an intact basal/myoepithelial cell layer but typical secretions, likely representing an in situ lesion in a preexisting duct. A similar feature has been documented in the paper by Huang et al.<sup>15</sup>

The tumor on the eyelid was unusual in that it had relatively few areas with typical closely packed lumina filled with secretions. The tumor instead was mainly composed of solid, papillary, and pseudopapillary areas with focal apocrine or colloid-like secretion. Similar lesions have been, however, reported both in the skin and salivary glands.<sup>7,13</sup> It is known that in some organs, for example, the thyroid glands, *ETV6-NTRK3* translocation was found in lesions that have different morphology from secretory carcinoma.<sup>26,27</sup> Because of colloid-like secretion, this case was stained for TTF1 but

proved negative. The patient did not have any evidence of a primary of the thyroid gland on a clinical work-up. Furthermore, the cells in this case in some areas were larger and had a blastoid appearance; however, we think this feature does not qualify for high-grade transformation, an event that has also been reported in extracutaneous secretory carcinomas.<sup>23,24</sup>

A purist can argue against considering the case with the nipple tumor as primary cutaneous. We, however, included this case on the basis of the fact that the lesion was superficial, confined to the nipple, and no breast parenchymal involvement was identified on a thorough work-up and, later, microscopically, following the mastectomy. It is known that some tumors typically occurring on the nipple, such as nipple adenoma, syringomatous adenoma, nodular mucinosis, and nipple pseudolymphoma, are covered by both dermatopathology and mammary pathology. Moreover, of interest is that this patient and another patient with a tumor in the axilla are the oldest individuals with secretory carcinoma ever reported (75 and 98 y, respectively).

In all but 1 case, *ETV6-NTRK3* translocation was found. In the remaining case, an *NFIX-PKNI* fusion was detected. The latter has been previously described in neither cutaneous secretory carcinoma nor in extracutaneous homonymous tumors. In fact, this fusion has not been reported at all, to the best of our knowledge. Nuclear factor I, X-type (*NFIX*) gene is

located on 19p13 and codes for a ubiquitous 47-kD dimeric DNA-binding protein, belonging to a family of transcription factors. Pathogenic variants of *NFIX* have also been reported as causative of Marshall-Smith Syndrome and Malan syndrome (Sotos syndrome 2).<sup>28,29</sup> The Protein kinase-1 (PKN1) gene is also located on 19p13 and codes for protein belonging to the protein kinase C superfamily that is activated by the Rho family of small G proteins and may mediate the Rho-dependent signaling pathway. Mutations in *PKN1* gene were described in rhabdomyosarcoma.<sup>30</sup>

Apart from the *ETV6-NTRK3* translocation, other gene fusions reported in secretory carcinoma in different organs include *ETV6-RET*, *ETV6-MET*, and dual fusion *ETV6-NTRK3* and *ETV6-MAML3*.<sup>7,31,32</sup> Cases of secretory carcinoma of the salivary gland with *NCOA4-RET* and *TRIM27-RET* gene fusions have subsequently been reclassified as intraductal carcinomas.<sup>31,33</sup>

In conclusion, we have described 6 new cases of secretory carcinoma involving the skin. Adding this series to the previously published 19 cases, it can be summarized that cutaneous secretory carcinoma mainly occurs in female individuals (female 16, male 9). The ages of the patients ranged from 13 to 98 years (mean: 51.8, median: 51.5). The most common location is the axilla (n = 10) followed by the neck (n = 3), and lip (n = 3). The tumors seem to follow an indolent course, without recurrence and metastasis. *ETV6-NTRK3* translocation has been identified in 22 of the 25 studied cases, and 1 case had a heterozygous deletion of *ETV6* in 25% of cells.<sup>11</sup> We extend the spectrum of translocations by reporting a novel *NFIX-PKN1* translocation and broaden the histopathologic spectrum by adding a case with a mucinous component.

## REFERENCES

- Skalova A, Vanecek T, Sima R, et al. Mammary analogue secretory carcinoma of salivary glands, containing the *ETV6-NTRK3* fusion gene: a hitherto undescribed salivary gland tumor entity. *Am J Surg Pathol*. 2010;34:599–608.
- Bishop JA, Taube JM, Su A, et al. Secretory carcinoma of the skin harboring *ETV6* gene fusions: a cutaneous analogue to secretory carcinomas of the breast and salivary glands. *Am J Surg Pathol*. 2017;41:62–66.
- Rosen PP, Cranor ML. Secretory carcinoma of the breast. *Arch Pathol Lab Med*. 1991;115:141–144.
- Rosen PP. *Rosen's Breast Pathology*, 3rd ed. Philadelphia, PA: Lippincott Williams and Wilkins; 2008.
- Kazakov DV, Michal M, Kacerovska D, et al. *Cutaneous Adnexal Tumors*. Philadelphia: Lippincott Williams and Wilkins; 2012:814.
- Majewska H, Skalova A, Stodulski D, et al. Mammary analogue secretory carcinoma of salivary glands: a new entity associated with *ETV6* gene rearrangement. *Virchows Arch*. 2015;466:245–254.
- Skalova A, Vanecek T, Martinek P, et al. Molecular profiling of mammary analogue secretory carcinoma revealed a subset of tumors harboring a novel *ETV6-RET* translocation: report of 10 cases. *Am J Surg Pathol*. 2018;42:234–246.
- Brandt SM, Swistel AJ, Rosen PP. Secretory carcinoma in the axilla: probable origin from axillary skin appendage glands in a young girl. *Am J Surg Pathol*. 2009;33:950–953.
- Amin SM, Beattie A, Ling X, et al. Primary cutaneous mammary analogue secretory carcinoma with *ETV6-NTRK3* translocation. *Am J Dermatopathol*. 2016;38:842–845.
- Chang MD, Arthur AK, Garcia JJ, et al. *ETV6* rearrangement in a case of mammary analogue secretory carcinoma of the skin. *J Cutan Pathol*. 2016;43:1045–1049.
- Albus J, Batanian J, Wenig BM, et al. A unique case of a cutaneous lesion resembling mammary analog secretory carcinoma: a case report and review of the literature. *Am J Dermatopathol*. 2015;37:e41–e44.
- Llamas-Velasco M, Mentzel T, Rutten A. Primary cutaneous secretory carcinoma: a previously overlooked low-grade sweat gland carcinoma. *J Cutan Pathol*. 2018;45:240–245.
- Bao Y, Li J, Zhu Y. Mammary analog secretory carcinoma with *ETV6* rearrangement arising in the conjunctiva and eyelid. *Am J Dermatopathol*. 2018;40:531–535.
- Hindocha N, Wilson MH, Pring M, et al. Mammary analogue secretory carcinoma of the salivary glands: a diagnostic dilemma. *Br J Oral Maxillofac Surg*. 2017;55:290–292.
- Huang S, Liu Y, Su J, et al. "Secretory" carcinoma of the skin mimicking secretory carcinoma of the breast: case report and literature review. *Am J Dermatopathol*. 2016;38:698–703.
- Moore RF, Cuda JD. Secretory carcinoma of the skin: case report and review of the literature. *JAAD Case Rep*. 2017;3:559–562.
- Kazakov DV, Hantschke M, Vanecek T, et al. Mammary-type secretory carcinoma of the skin. *Am J Surg Pathol*. 2010;34:1226–1227.
- Hycza MD, Ng T, Crawford RI. Detection of the *ETV6-NTRK3* translocation in cutaneous mammary-analogue secretory carcinoma. *Diagn Histopathol*. 2015;21:481–484.
- Nguyen JK, Bridge JA, Joshi C, et al. Primary mammary analog secretory carcinoma (MASC) of the vulva with *ETV6-NTRK3* fusion: a case report. *Int J Gynecol Pathol*. 2019;38:283–287.
- Viswanatha DS, Foucar K, Berry BR, et al. Blastic mantle cell leukemia: an unusual presentation of blastic mantle cell lymphoma. *Mod Pathol*. 2000;13:825–833.
- Gaffney R, Chakerian A, O'Connell JX, et al. Novel fluorescent ligase detection reaction and flow cytometric analysis of *SYT-SSX* fusions in synovial sarcoma. *J Mol Diagn*. 2003;5:127–135.
- Antonescu CR, Kawai A, Leung DH, et al. Strong association of *SYT-SSX* fusion type and morphologic epithelial differentiation in synovial sarcoma. *Diagn Mol Pathol*. 2000;9:1–8.
- Skalova A, Vanecek T, Majewska H, et al. Mammary analogue secretory carcinoma of salivary glands with high-grade transformation: report of 3 cases with the *ETV6-NTRK3* gene fusion and analysis of *TP53*, *beta-catenin*, *EGFR*, and *CCND1* genes. *Am J Surg Pathol*. 2014;38:23–33.
- Xu B, Aryequeaye R, Wang L, et al. Sinonasal secretory carcinoma of salivary gland with high grade transformation: a case report of this under-recognized diagnostic entity with prognostic and therapeutic implications. *Head Neck Pathol*. 2018;12:274–278.
- Skalova A, Gnepp DR, Lewis JS Jr, et al. Newly described entities in salivary gland pathology. *Am J Surg Pathol*. 2017;41:e33–e47.
- Petersson F, Michal M, Kazakov DV, et al. A new hitherto unreported histopathologic manifestation of mammary analogue secretory carcinoma: "Masked MASC" associated with low-grade mucinous adenocarcinoma and low-grade in situ carcinoma components. *Appl Immunohistochem Mol Morphol*. 2016;24:e80–e85.
- Dogan S, Wang L, Ptashkin RN, et al. Mammary analog secretory carcinoma of the thyroid gland: a primary thyroid adenocarcinoma harboring *ETV6-NTRK3* fusion. *Mod Pathol*. 2016;29:985–995.
- Aggarwal A, Nguyen J, Rivera-Davila M, et al. Marshall-Smith syndrome: novel pathogenic variant and previously unreported associations with precocious puberty and aortic root dilatation. *Eur J Med Genet*. 2017;60:391–394.
- Martinez F, Marin-Reina P, Sanchis-Calvo A, et al. Novel mutations of *NFIX* gene causing Marshall-Smith syndrome or Sotos-like syndrome: one gene, two phenotypes. *Pediatr Res*. 2015;78:533–539.
- Chen L, Shern JF, Wei JS, et al. Clonality and evolutionary history of rhabdomyosarcoma. *PLoS Genet*. 2015;11:e1005075.
- Guilmette J, Dias-Santagata D, Nose V, et al. Novel gene fusions in secretory carcinoma of the salivary glands: enlarging the *ETV6* family. *Hum Pathol*. 2019;83:50–58.
- Rooper LM, Karantanos T, Ning Y, et al. Salivary secretory carcinoma with a novel *ETV6-MET* fusion: expanding the molecular spectrum of a recently described entity. *Am J Surg Pathol*. 2018;42:1121–1126.
- Skalova A, Vanecek T, Uro-Coste E, et al. Molecular profiling of salivary gland intraductal carcinoma revealed a subset of tumors